



Contents lists available at ScienceDirect

Tetrahedron: Asymmetry

journal homepage: www.elsevier.com/locate/tetasy

Mesoporous SBA-15-supported chiral catalysts: preparation, characterization and asymmetric catalysis

Guohua Liu*, Mouming Liu, Yunqiang Sun, Jianyao Wang, Chuanshou Sun, Hexing Li*

Department of Chemistry, College of Life and Environmental Science, Shanghai Normal University, Shanghai 200234, PR China

ARTICLE INFO

Article history:

Received 6 December 2008

Accepted 9 January 2009

Available online 13 February 2009

ABSTRACT

Two mesoporous silica-supported chiral Rh and Ru catalysts **5** and **6** with ordered two-dimensional hexagonal mesostructures were prepared by directly postgrafting organometallic complexes $\text{RhCl}[(R)\text{-MonoPhos}(\text{CH}_2)_3\text{Si}(\text{OMe})_3][(R,R)\text{-DPEN}]$ and $\text{RuCl}_2[(R)\text{-MonoPhos}(\text{CH}_2)_3\text{Si}(\text{OMe})_3][(R,R)\text{-DPEN}]$ (DPEN = 1,2-diphenylethylenediamine) on SBA-15. During the asymmetric hydrogenation of various aromatic ketones under 40 atm H_2 , both catalysts exhibited high catalytic activities (more than 97% conversions) and moderate enantioselectivities (33–54% ee). Furthermore, the chiral Rh catalyst **5** could be easily recovered and used repetitively five times without significantly affecting its catalytic activity and enantioselectivity. A catalytic comparison of the mesoporous silica-supported chiral Rh catalyst **4** prepared by a postmodification method is also discussed.

Crown Copyright © 2009 Published by Elsevier Ltd. All rights reserved.

1. Introduction

The incorporation of chiral ligand or catalyst on mesoporous silica materials for asymmetric catalysis has attracted a great deal of interest due to its tunable pore dimension, well-defined pore arrangement, relatively large specific surface area and pore volume.¹ The large specific surface area and pore volume can enhance the loading amounts of the metal catalyst and increase its catalytic efficiency, while the tunable pore dimension and well-defined pore arrangement can avoid the aggregation of catalytic active species and maintain excellent stereocontrol performance. More importantly, these mesoporous silica-supported chiral catalysts do not swell or dissolve in common organic solvents, they are easy and reliable to be reused via simple precipitation or nanofiltration methods. Furthermore, they also exhibit superior thermal and mechanical stability in catalytic process, showing a potential application in industry. In general, the incorporation of ligand or organometallic complex on mesoporous silica materials can be achieved by either a postgrafting (a postsynthesis method)² or a co-condensation method (a direct synthesis method).³ Although the co-condensation method shows a significant advantage with a more uniform distribution and a higher loading amount, such a direct synthesis method often results in an ill-ordered mesostructure of materials. Furthermore, because catalysts prepared by a co-condensation method utilize an in situ coordination strategy for catalysis, it often meets the challenges on how to effectively coordinate the organometallic complex under a catalytic process and to maintain the suitable microenvironment of catalytic active sites on

mesoporous silica materials. It is also difficult to eliminate the negative effect derived from the other organic ligands on the materials by the in situ coordination strategy, which often plays a key role in asymmetric catalysis. Compared with the co-condensation method, the postgrafting method involves operationally simple techniques and is well known to maintain highly ordered mesostructure of materials. More importantly, the direct incorporation of organometallic catalyst on mesoporous silica materials via the postgrafting method can maintain its active structure and eliminate a variety of uncontrollable factors, resulting in a high enantioselectivity.

Optically active BINOL-derived monodonor phosphorus ligand MonoPhos⁴ and 1,2-diphenylethylenediamine (DPEN)⁵ are two kinds of important chiral ligands, which are used extensively to generate highly enantioselective catalysts for asymmetric hydrogenation of ketones. (R)-MonoPhos has a significant advantage because it is much less expensive than chiral bidentate ligands such as BINAP, while (R,R)-DPEN has been well known to be incorporated onto supports such as polymer and inorganic materials.⁶ More importantly, some of which have successively been incorporated onto various mesoporous supports.^{6d,e} These pioneering works not only offer synthetic methods for chiral ligand, but also explore immobilized strategies for incorporation of chiral ligand or catalyst on mesoporous silica materials. Recently, Li et al. reported a series of mesoporous chiral Rh catalysts using analogues [(1R,2R)-1,2-cyclohexanediamine] of (R,R)-DPEN as chiral ligand via a co-condensation method, and applied them to the asymmetric transfer hydrogenation of acetophenone.^{3e,f} Although these catalysts with ethane group bridging in the mesoporous framework exhibit higher catalytic activity and enantioselectivity than the with corresponding mesoporous silicas, they still give the worse

* Corresponding authors. Tel.: +86 21 64321819; fax: +86 21 64322511 (G.L.).
E-mail addresses: gqliu@shnu.edu.cn (G. Liu), HeXing-Li@shnu.edu.cn (H. Li).

enantioselectivities than the corresponding homogeneous catalysts due to the in situ coordination in catalytic process. Our group also reported two types of Ru(or Ir)-SBA-15/(*R,R*)-DPEN catalysts, in which (*R,R*)-DPEN was incorporated onto SBA-15 support via a postgrafting method.⁷ It was found that both catalysts exhibit higher enantioselectivities than those corresponding homogeneous catalysts in the asymmetric hydrogenation of aromatic ketones, in which the chiral inductivity of the catalysts protruding into the pore of the mesoporous materials could also be enhanced by this kind of postgrafting method. Apparently, the direct incorporation of organometallic catalyst on mesoporous silica materials via a direct postgrafting method represents a promising strategy in the field of asymmetric catalysis.

We are currently interested in the mesoporous silica-supported catalysts,^{7,8} especially, the direct incorporation of organometallic complexes on mesoporous silica materials.⁷ As an extension of our previous studies, we herein report a synthesis of two mesoporous silica-supported chiral catalysts based on the SBA-15 via a postgrafting method, and apply them to the asymmetric hydrogenation of ketones. The key feature is that we employ an organic silica resource containing (*R*)-MonoPhos ligand, and then directly incorporate its homogeneous organometallic catalyst $MCl_n[(R)\text{-MonoPhos}][(\text{R,R})\text{-DPEN}]$ onto mesoporous silica materials by a postgrafting method. Such mesoporous silica-supported catalysts not only maintain the highly ordered mesostructure of materials, but also allow catalyst **5** to be easily recovered and used repetitively without significantly affecting its catalytic activity and enantioselectivity. Meanwhile, these studies provide an opportunity to investigate the role of the mesoporous silica materials as supports in asymmetric catalysis (Scheme 1).

2. Results and discussion

2.1. Structural and morphological properties of the catalysts

The FTIR spectra of catalysts **5** and **6** are shown in Figure 1. The catalysts **5** and **6** displayed generally characteristic bands of pure SBA-15 around 3440, 1634, 1070, 804, and 458 cm^{-1} for $\nu(\text{O-H})$, $\delta(\text{O-H})$, $\nu(\text{Si-O})$, $\omega(\text{O-H})$, and $\delta(\text{Si-O})$, respectively. The weak peaks

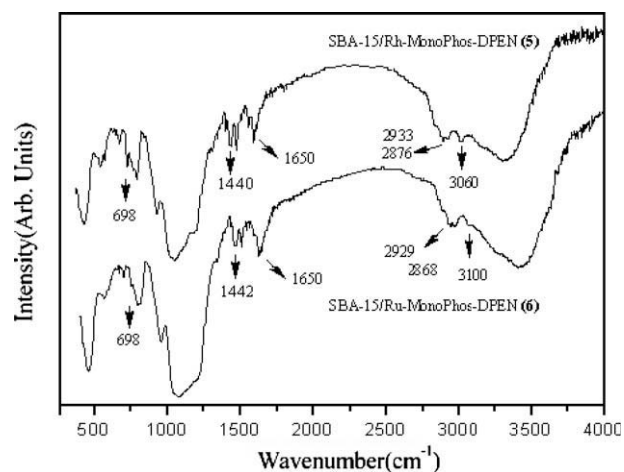
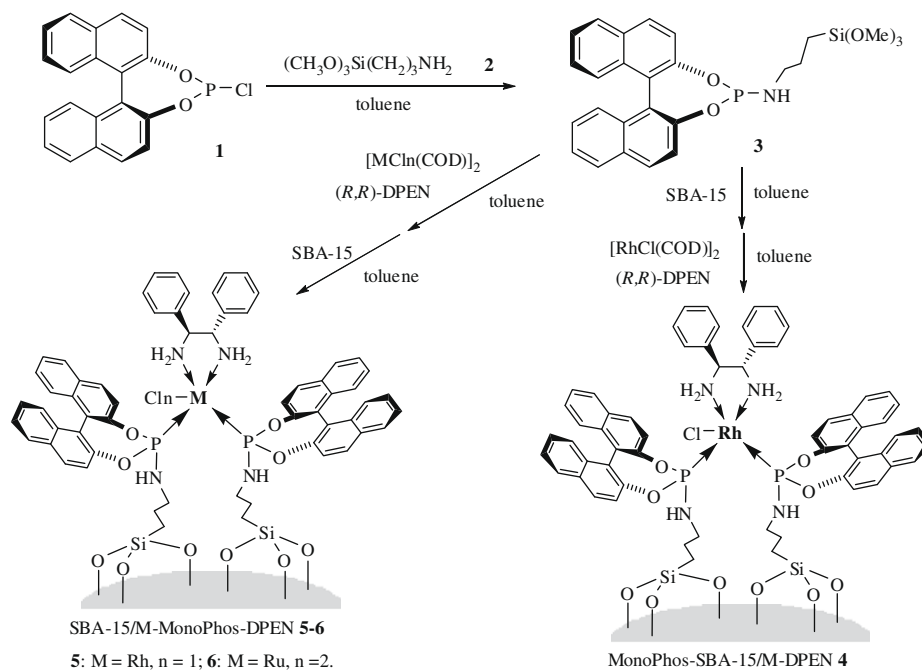


Figure 1. FTIR spectra of catalysts **5** and **6**.

of catalysts **5** and **6** at 3100–2800 cm^{-1} were assigned to the asymmetric and symmetric stretching vibrations of C–H bonds,⁹ while the weak peak around 698 cm^{-1} was ascribed to the characteristic peak of H out-of-plane deformation of substituted benzene ring.¹⁰ All these relatively weak peaks derived from the organometallic complexes demonstrate the successful incorporation of organometallic complexes onto the SBA-15. The peak indicative of $\nu(\text{Si-C})$ and $\nu(\text{P-O})$ should appear at around 1100 cm^{-1} . However, it was difficult to distinguish because of an overlap by absorbance from $\nu(\text{Si-O})$ in the SBA-15.^{9,10b} In comparison to the pure SBA-15, catalysts **5** and **6** displayed an abrupt decrease in band intensity at 3400 cm^{-1} , which further demonstrated substitution of a large fraction of surface OH groups by the organometallic complexes.

The incorporation of the organometallic complexes onto the pure SBA-15 could be further confirmed by solid-state NMR spectra. As shown in Figure 2a, the ^{29}Si MAS NMR spectra of catalysts **5** and **6** showed two groups of peaks with four oxygen neighbors (Q-type species) and with three oxygen neighbors (T-type species), respectively. The Q-type species were desired from TEOS, whereas



Scheme 1. Synthesis of the mesoporous silica-supported chiral catalysts **5** and **6**.

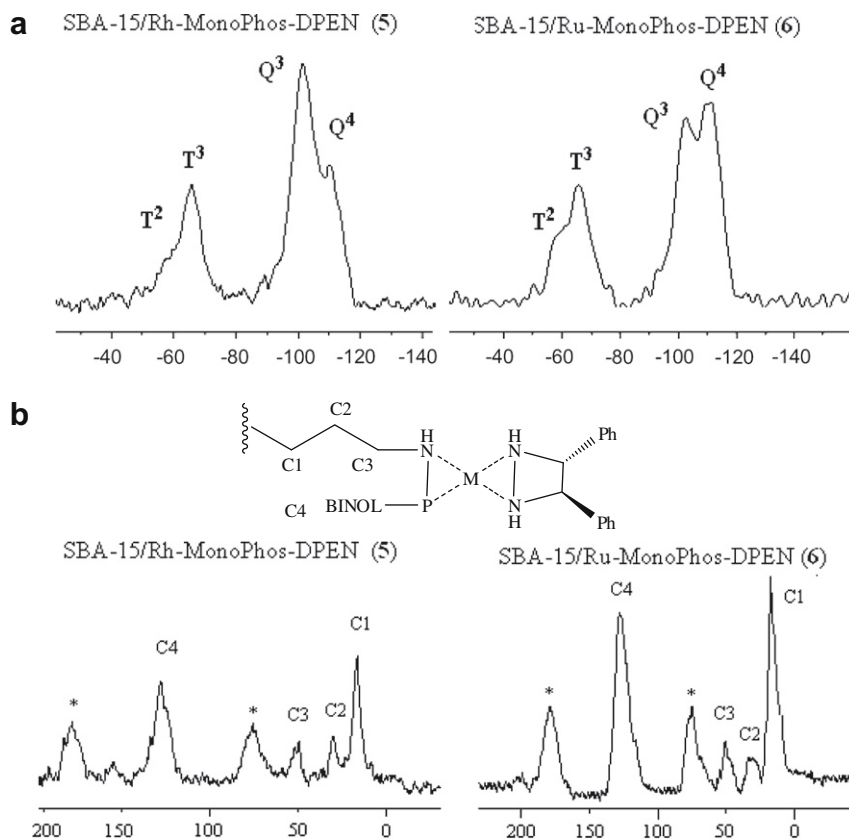


Figure 2. NMR spectra of the catalysts **5** and **6** (a) ^{29}Si MAS NMR and (b) ^{13}C CP MAS NMR.

the T-type species were derived from silylether groups. Typical isomer shift values were $-91.5/-101.5/-110$ ppm for Q²/Q³/Q⁴ signals (Q²{(HO)₂Si(OSi)₂}, Q³{(HO)Si(OSi)₃}, Q⁴{Si(OSi)₄}) and $-48.5/-58.5/-67.5$ ppm for T¹/T²/T³ signals (T¹{R(HO)₂SiOSi}, T²{R(HO)Si(OSi)₂}, T³{RSi(OSi)₃}).¹¹ Catalyst **5** showed two strong Q signals corresponding to Q⁴ ($\delta = -111$ ppm) and Q³ ($\delta = -101$ ppm), and two T signals for T³ ($\delta = -66$ ppm) and T² ($\delta = -57$ ppm). The corresponding signals appeared in -112 (Q⁴), -103 (Q³) ppm and -67 (T³), -58 (T²) ppm for catalyst **6**. These relatively strong Q³ and Q⁴ signals suggested that the catalysts **5** and **6** mainly possessed network structures of (HO)Si(OSi)₃ and {Si(OSi)₄}, while the weak T² and T³ signals indicated the formation of {R(HO)Si(OSi)₂} and RSi(OSi)₃ (R = organometallic complexes) as a part of wall in mesoporous structures.¹¹ ^{13}C CP MAS NMR spectra displayed the peaks at 127, 49, 31, 12 ppm in the catalyst **5**, and at 125, 49, 32, 12 ppm in the catalyst **6**, corresponding to aromatic and aliphatic carbon atoms, as marked in Figure 2b.

Figure 3 shows XRD patterns of the catalysts **5** and **6**. Similar to pure SBA-15, catalysts **5** and **6** also exhibited one similar intense d_{100} diffraction and two similar weak peaks indicative of d_{110} and d_{200} diffractions, implying that ordered dimensional-hexagonal mesostructure ($p6mm$) could be well preserved.¹² The reduced peak intensity suggested that the incorporation of the organometallic complexes onto the pure SBA-15 might disturb the ordered dimensional-hexagonal mesostructure by a certain degree. TEM images in Figure 4 further confirmed the ordered mesostructure in catalysts **5** and **6**.

Nitrogen adsorption-desorption isotherms of catalysts **5** and **6** are shown in Figure 5. Similar to pure SBA-15, catalysts **5** and **6** exhibited typical IV type N₂ adsorption-desorption isotherms with H₁ hysteresis loop and a visible step at $P/P_0 = 0.40-0.70$, corresponding to the capillary condensation of nitrogen in mesopores.

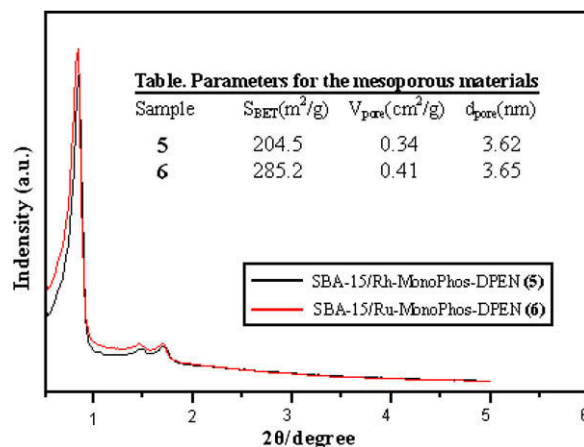


Figure 3. Powder XRD patterns of the catalysts **5** and **6**.

The changes in hysteresis could be attributed to different hydrolysis and condensation rates between the pure SBA-15 and the organometallic complexes.¹³ As the structural parameters show in Figure 3, the incorporation of organometallic complexes onto SBA-15 caused a decrease in mesopore size, surface area, and pore volume, obviously due to a coverage of pore surface with the organometallic complexes, leading to an increase in the wall thickness and even partial blockage of the mesoporous channels.⁷

2.2. Catalytic properties of the mesoporous materials

The contents of the organometallic complexes in catalysts **5** and **6** were calculated from elemental analyses. Elemental analyses of

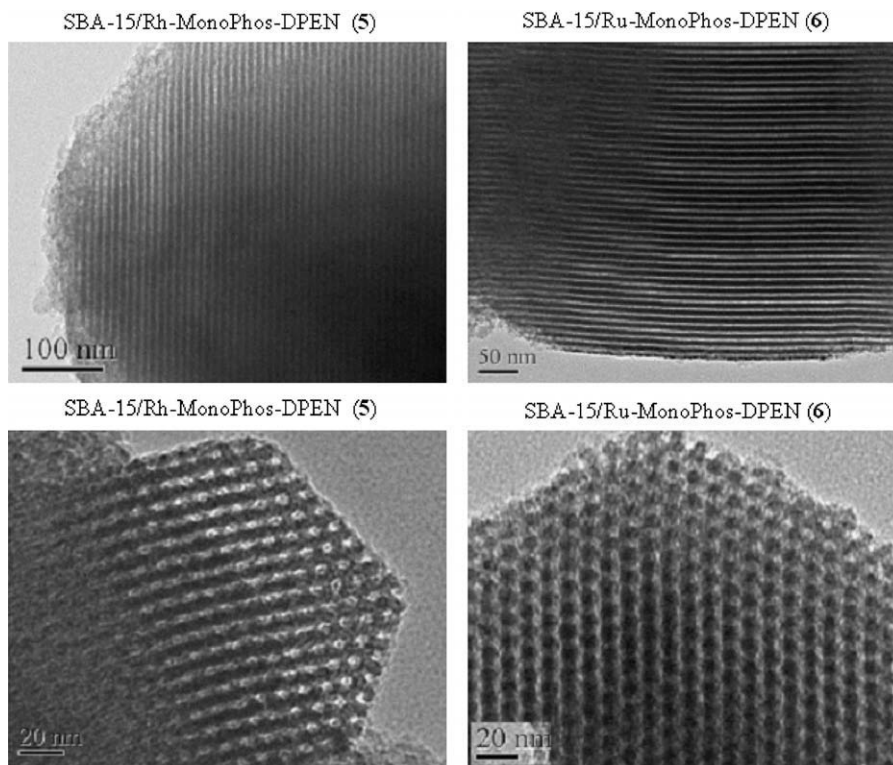


Figure 4. The TEM images of the catalysts **5** and **6** viewed along [100] and [001] directions.

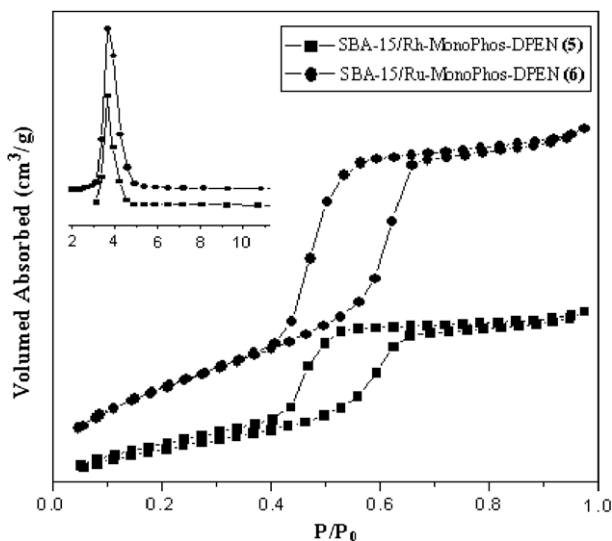


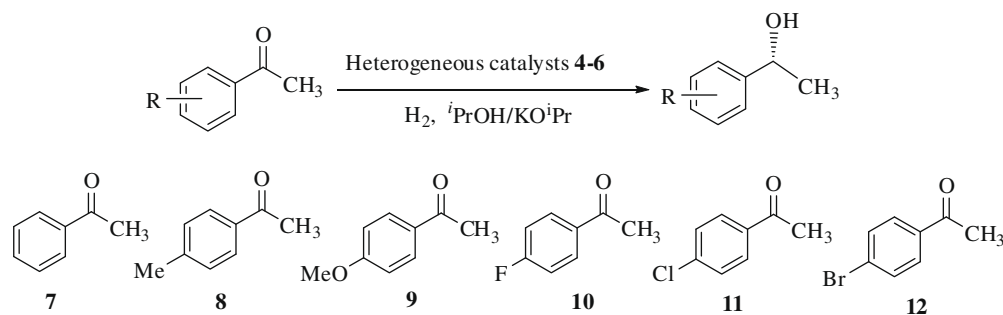
Figure 5. Nitrogen adsorption–desorption isotherms of the catalysts **5** and **6**.

catalysts **5** and **6** calculated from mass% of N (0.30% and 0.29%) showed that the loading amounts of the nitrogen atoms were 0.214 and 0.207 mmol per gram catalyst. When comparing the data of the ICP analyses, the Rh and Ru loading amounts [5.46 and 5.22 mg (0.053 and 0.052 mmol) per gram catalyst from ICP analyses] in catalysts **5** and **6** suggested that there were four nitrogen atoms in each organometallic complex, indicating that 1 equiv of MonoPhos moieties and 1 equiv of DPEN moiety coordinated one metal atom. Such a structural arrangement is consistent with the structure reported in the literature.¹⁴ In addition, when comparing the metal loading amounts in the catalysts **5** and **6** with the theoretical initial values, it was found that about 30 mol % of

the organometallic complexes could be incorporated onto the mesoporous organosilicas. Increasing the amounts of organometallic complexes in the initial gel mixture did not result in an increase in the loading amounts, suggesting that such loading amounts in catalysts **5** and **6** had reached maximum values.

The asymmetric hydrogenation of prochiral ketones is an important method to prepare enantiomerically pure secondary alcohols, which were very valuable synthetic intermediates for pharmaceuticals or materials. Recently, a variety of homogeneous chiral Ru and Rh catalysts have been demonstrated to be highly enantioselective in the hydrogenation of prochiral ketones.^{5,14,15} With two mesoporous silica-supported catalysts on hand, we chose the asymmetric hydrogenation of aromatic ketones as probe to evaluate their catalytic activities and enantioselectivities. According to the reported method,^{14a} 2-propanol was used as the optimal solvent, and potassium isopropoxide as the base. A typical asymmetric transfer hydrogenation reaction was performed in a stirred suspension of catalyst **5** or **6** (2.00 μ mol, metal amounts based on the ICP analysis) in *i*-PrOH (5 mL) containing a ketone substrate in the presence of potassium isopropoxide system under 40 atm H₂ at 50 °C for 16 h. After the reaction, the organic layer was concentrated and purified by flash chromatography for homogeneous systems or was filtered to separate the catalysts for heterogeneous systems. The preliminary results are summarized in Table 1. In general, the high conversions and no side products, and moderate enantioselectivities were obtained in the asymmetric hydrogenation of aromatic ketones under 40 atm H₂. Taking acetophenone as an example, catalyst **5** provided (*S*)-1-phenyl-1-ethanol with more than 99% conversion and 53.8% ee (entry 2), while catalyst **6** gave the corresponding alcohol with more than 99% conversion and 48.0% ee (entry 15). It is interesting to note that both catalysts offered an (*S*)-enantiomer, which could ascribe intrinsic (*S*)-selectivity of this phosphorous ligand with (*R*)-selectivity of the diamine.^{15a} Furthermore, it was also found that both enantioselectivities were better than those obtained with the cor-

Table 1
Asymmetric hydrogenation of aromatic ketones under H₂ pressure^a



Entry	Substrate	Catalyst	Run	Time	Conv. ^b (%)	ee ^b (%)
1	7	5	1	4	>99	53.0 ^c
2	7	5	1	16	>99	53.8
3	8	5	1	16	>99	43.8
4	9	5	1	16	97.6	41.7
5	10	5	1	16	>99	43.4
6	11	5	1	16	>99	47.8
9	12	5	1	16	>99	46.0
7	7	3 + [RhCl(COD)] ₂	1	16	>99	5.4
8	7	4	1	16	54.9	30.8
10	7	5	2	16	>99	53.6 ^d
11	7	5	3	16	>99	52.4 ^d
12	7	5	4	16	98.5	47.0 ^d
13	7	5	5	16	99.5	46.3 ^d
14	7	6	1	4	>99	43.6 ^c
15	7	6	1	16	>99	48.0
16	8	6	1	16	>99	41.7
17	9	6	1	16	>99	37.6
18	10	6	1	16	>99	43.2
19	11	6	1	16	>99	33.2
20	12	6	1	16	>99	35.2
21	7	6	2	16	96.6	39.9 ^d
22	7	6	3	16	>99	32.6 ^d
23	7	6	4	16	>99	29.8 ^d

^a Reactions were carried out in *i*-PrOH. Reaction conditions: catalyst (2.00 μmol of Rh or Ru based on the ICP analysis), *i*-PrOH (5 mL), *i*-PrOK (5 mL), ketone (0.4 mmol), reaction temperature (50 °C), reaction time (16 h), argon atmosphere.

^b Determined by chiral GC analysis. The absolute configuration of the product is (*S*).

^c Data were obtained using the homogeneous catalysts.

^d Recovered catalysts were used.

responding homogeneous catalysts (entry 1 vs entry 2 and entry 14 vs entry 15), although the latter are slightly lower than that of the 54% ee obtained with the parent catalyst, [(MonoPhos)RuCl₂((*R,R*)-DPEN)], reported in the literature.^{14a} The higher enantioselectivities of catalysts **5** and **6** than the corresponding homogeneous catalysts could be attributed to the regularly dispersive arrangement of the catalytic species on mesoporous silica materials, in which this type of arrangement not only offered reasonable space for the chiral recognition of substrate, but also restricted the aggregation or disorder of the catalytic species, resulting in higher ee values. On the basis of the reaction conditions, catalysts **5** and **6** were further investigated using a series of aromatic ketones as substrates (entries 3–9 and 16–20). It was found that the structures and electronic properties of substituents in the acetophenone did not significantly affect the enantioselectivity. Only slight changes in enantioselectivities were observed with a change of the substituents in the acetophenone.

In order to explore the nature of the heterogeneous catalysis, two control experiments were also carried out using **3** plus [RhCl(COD)]₂ and **4** prepared by a postmodification method as catalysts under similar reaction conditions. It was found that the former afforded the corresponding alcohol in more than 99%

conversion and 5.4% ee value, while the latter gave the corresponding alcohol only in 54.9% conversion and 30.8% ee (entry 2 vs entries 7 and 8). The former suggested that the enantioselectivity was generated from [(*R*)-MonoPhos-Rh-(*R,R*)-DPEN] rather than from [(*R*)-MonoPhos-Rh], while the latter indicated that the catalyst was synthesized by a postmodification method resulting in a worse catalytic performance. When catalysts **4** with **5** were compared, the low enantioselective activity of **4** might be due to that the postmodified organic groups [(*R,R*)-DPEN] were mainly near the pore mouth because of the mass transfer.¹⁶ Similar phenomena were also observed in our previous reports.⁷

As organometallic metal in most solid-supported catalysts was easy to be leached during the catalytic process, we also evaluated the catalytic property of solid catalyst **5** in order to test effect of leached catalysts probably derived from physical absorption. After completion of the reaction, catalyst **5** was removed from the reaction mixture via simple filtration, followed by a thorough Soxhlet extraction in toluene solvent for 12 h. It was found that the reused catalyst **5** still afforded more than 99% conversion and almost same ee values (entry 2 vs entry 10). The result suggested that the homogeneous catalyst was immobilized onto mesoporous silica materials via covalent bonding rather than via physical absorption. More

importantly, such a catalyst could be recovered and reused five times without obviously affecting the ee value, showing a good application in industry. ICP analysis further confirmed the fact that the content of Rh after fifth recycle was 5.39 mg per gram catalyst, in which the lost Rh loading amounts could be neglected.

3. Conclusion

In conclusion, we have presented a facile approach to prepare mesoporous silica-supported chiral Rh and Ru catalysts **5** and **6** by directly anchoring the organometallic complexes onto SBA-15, which exhibited high catalytic activities and moderate enantioselectivities during the asymmetric hydrogenation of various aromatic ketones under 40 atm H₂. Both catalysts showed higher activities and enantioselectivities than the corresponding homogeneous catalysts. Furthermore, catalyst **5** could be recovered and reused five times without affecting the ee value, showing a possibility in industrial applications.

4. Experimental

4.1. Synthesis of **3**

Under an argon atmosphere, to a stirred solution of **1** (0.50 g, 1.43 mmol) and triethylamine (0.13 mL, 2.15 mmol) in 3 mL dry toluene was added a solution of **2** (0.26 g, 1.45 mmol) in 3 mL dry toluene at 0 °C. The resulting mixture was then allowed to warm to room temperature slowly and was stirred for another 3 h. After the solvent was removed in vacuo, the residue was passed fast through a short column (silica gel, eluent: Et₃N/hexane/CH₂Cl₂ = 1:10:40) and concentrated in vacuo to afford **3** as beige glass. Yield: 56%; $[\alpha]_D^{20} = -548.6$ (c 0.61, toluene); ¹H NMR (400 MHz, CDCl₃): δ 7.95–7.60 (m, 8H), 7.95–7.60 (t, J = 7.2 Hz, 2H), 7.00–6.90 (t, J = 7.2 Hz, 2H), 3.59 (s, 9H), 2.62 (t, J = 5.4 Hz, 2H), 2.08 (s, 1H, NH), 1.56–1.50 (m, 2H), 0.62 (t, J = 5.4 Hz, 2H); ¹³C NMR (126 MHz, CDCl₃): δ 6.9, 26.1, 43.3, 50.3, 113.6, 118.5, 123.5, 124.4, 127.1, 128.0, 129.2, 130.5, 134.1, 153.2; IR: 3399, 3098, 2986, 2945, 1621, 1586, 1508, 1462, 1215, 1084, 1022, 975, 821, 745 cm⁻¹; ³¹P NMR (162 MHz, CDCl₃): δ 150.20; ESI-HRMS, calcd for C₂₆H₂₈NO₅PSi, 493.1573, found 493.1582.

4.2. Catalyst preparation

A typical procedure is as follows: Under an argon atmosphere, to a stirred solution of **3** (0.208 g, 0.420 mmol) and (R,R)-DPEN (0.045 g, 0.210 mmol) in 3 mL dry toluene was added [Rh(COD)Cl]₂ (0.052 g, 0.104 mmol). The resulting mixture was stirred at room temperature for 3 h. Then pure siliceous support [SBA-15 (pore size of 7.6), 1.0 g] and dry toluene (25 mL) were added to the above solution. The resulting mixture was stirred and refluxed for 24 h, after which the residues were filtered and washed twice with dry toluene. After Soxhlet extraction in a toluene solvent to remove homogeneous and unreacted starting materials, the solid was dried under reduced pressure overnight to afford SBA-15/Rh-MonoPhos-DPEN **5** (1.078 g, 29.2% relative to **3**) as a light yellow powder. IR 3440, 3060, 2965, 2933, 2876, 1645, 1634, 1621, 1600, 1507, 1458, 1440, 1213, 1070, 955, 812, 804, 739, 694, 563, 457 cm⁻¹; Elemental analysis (%): C, 4.29; H, 1.36; N, 0.30; *d*_{pore}: 3.62 nm; *S*_{BET}: 204.5 m²/g. ²⁹Si MAS/NMR (300 MHz): Q⁴ (δ = -111 ppm), Q³ (δ = -101 ppm), T³ (δ = -66 ppm), T² (δ = -57 ppm); ¹³C CP/MAS (161.9 MHz): 127, 49, 31, 12 ppm; ³¹P CP MAS NMR (161.9 MHz): 193.3 ppm.

Catalyst 6: Prepared according to the general procedure described above. Light red powder (Yield: 28.5%); IR 3400, 3100, 2960, 2929, 2868, 1650, 1634, 1622, 1580, 1510, 1462, 1442,

1070, 951, 816, 805, 747, 698, 596, 458 cm⁻¹; Elemental analysis (%): C, 4.03; H, 1.28; N, 0.29; *d*_{pore}: 3.65 nm; *S*_{BET}: 285 m²/g. ²⁹Si MAS/NMR (300 MHz): Q⁴ (δ = -112 ppm), Q³ (δ = -103 ppm), T³ (δ = -67 ppm), T² (δ = -58 ppm); ¹³C CP/MAS (161.9 MHz): 125, 49, 32, 12 ppm; ³¹P CP MAS NMR (161.9 MHz): 196.5 ppm.

4.3. Characterization

Ru and Rh loading amounts in the catalysts were analyzed using an inductively coupled plasma optical emission spectrometer (ICP, Varian VISTA-MPX). X-ray powder diffraction (XRD) experiments were carried out on a Rigaku D/Max-RB diffractometer with Cu Kα radiation. Transmission electron microscopy (TEM) studies were performed on a JEOL JEM2010 electron microscope, operated at an acceleration voltage of 200 kV. Fourier transform infrared (FTIR) spectra were collected on a Nicolet Magna 550 spectrometer using KBr method. Nitrogen adsorption isotherms were measured at 77 K after being outgassed at 423 K overnight on a Quantachrome Nova 4000 analyzer. Pore size distributions and specific surface areas (*S*_{BET}) were calculated using BJH model and BET method, respectively. Liquid-state ¹H NMR, ¹³C NMR and ³¹P NMR, and Solid-state ²⁹Si MAS NMR and ¹³C CP MAS NMR spectra were recorded on a Bruker AV-400 spectrometer.

4.4. Catalytic reaction

A typical procedure is as follows: Solid catalyst **5** (37.7 mg, 2.00 μmol based on Rh from ICP) was added to a stainless-steel autoclave at room temperature in glovebox, into which anhydrous 2-propanol (5 mL, 0.065 mol), potassium isopropoxide (5 mL, 0.065 mol), and ketone (0.4 mmol) were charged beforehand. The hydrogenation was performed at 50 °C under 40 atm H₂ for 16 h. After completion of the reaction, hydrogen was carefully released. Dry CH₂Cl₂ (1 mL) was added, and the mixture was stirred for 1 min, after which the reactor contents were centrifuged (2000 r/min) for 1–2 min. The solution was purified by column chromatography (2 in. × 12 in. silica column) using ether as eluent. The main fractions were concentrated to afford a mixture of the ketone and the corresponding secondary alcohol as a colorless liquid to determine conversion and enantiomeric excess via a GC analysis using a Supelco β-Dex 120 chiral column (30 m × 0.25 mm (i.d.), 0.25 μm film).

Acknowledgments

We are grateful to China National Natural Science Foundation (20673072), Shanghai Sciences and Technologies Development Fund (071005119, S30406, and 07dz22303), and Shanghai Municipal Education Commission (08YZ71 and DZL807) for financial supports.

References

- (a) Thomas, J. M.; Raja, R. *Acc. Chem. Res.* **2008**, *41*, 708; (b) Heitbaum, M.; Glorius, F.; Escher, I. *Angew. Chem., Int. Ed.* **2006**, *45*, 4732; (c) Bein, T. *Curr. Opin. Solid State Mater. Sci.* **1999**, *4*, 85; (d) Li, C.; Huidong Zhang, H. D.; Jiang, D. M.; Yang, Q. H. *Chem. Commun.* **2007**, 547.
- (a) Mercier, L.; Pinnavaia, T. J. *Adv. Mater.* **1997**, *9*, 500; (b) Feng, X.; Fryxell, G. E.; Wang, L. Q.; Kim, A. Y.; Liu, J.; Kemmer, K. M. *Science* **1997**, *276*, 923; (c) Shepard, D. S.; Zhou, W.; Maschmeyer, T.; Matters, J. M.; Roper, C. L.; Parsons, S.; Johnson, B. F. G.; Duer, M. J. *Angew. Chem., Int. Ed.* **1998**, *37*, 2719.
- (a) Moller, K.; Bein, T.; Fischer, R. X. *Chem. Mater.* **1999**, *11*, 665; (b) Sims, S. D.; Burkett, S. L.; Mann, S. *Mater. Res. Soc. Symp. Proc.* **1996**, *431*, 77; (c) Macquarrie, D. J. *Chem. Commun.* **1996**, 1961; (d) Babonneau, F.; Leite, L.; Fontlupt, S. J. *Mater. Chem.* **1999**, *9*, 175; (e) Jiang, D. M.; Yang, Q. H.; Yang, J.; Zhang, L.; Zhu, G. R.; Su, W. G.; Li, C. *Chem. Mater.* **2005**, *17*, 6154; (f) Jiang, D. M.; Gao, J. S.; Yang, Q. H.; Yang, J.; Li, C. *Chem. Mater.* **2006**, *18*, 6012.
- (a) Feringa, B. L. *Acc. Chem. Res.* **2000**, *33*, 346; (b) Pena, D.; Minnaard, A. J.; de Vries, J. G.; Feringa, B. L. *J. Am. Chem. Soc.* **2002**, *124*, 14552; (c) Claver, C.; Fernandez, E.; Gillon, A.; Heslop, K.; Hyett, D. J.; Martorelli, A.; Orpen, A. G.;

- Pringle, P. G. *Chem. Commun.* **2000**, 961; (d) Reetz, M. T.; Goossen, L. J.; Meiswinkel, A.; Paetzold, J.; Feldthusen Jensen, J. *Org. Lett.* **2003**, *5*, 3099; (e) Jia, X.; Li, X.; Shi, Q.; Yao, X.; Chan, A. S. C. *J. Org. Chem.* **2003**, *68*, 4539; (f) Hannen, P.; Militzer, H. C.; Vogl, E. M.; Rampf, F. A. *Chem. Commun.* **2003**, 2210; (g) Gergely, I.; Hegedus, C.; Gulyas, H.; Szollosy, A.; Monsees, A.; Riermeier, T.; Bakos, J. *Tetrahedron: Asymmetry* **2003**, *14*, 1087; (h) Tang, W. J.; Huang, Y. Y.; He, Y. M.; Fan, Q. F. *Tetrahedron: Asymmetry* **2006**, *17*, 536; (i) Komarov, I. V.; Börner, A. *Angew. Chem., Int. Ed.* **2001**, *40*, 1197; (j) Simons, C.; Hanefeld, U.; Arends, I. W. C. E.; Maschmeyer, T.; Sheldon, R. A. *J. Catal.* **2006**, 239, 212.
5. (a) Fujii, A.; Hashiguchi, S.; Uematsu, N.; Ikariya, T.; Noyori, R. *J. Am. Chem. Soc.* **1996**, *118*, 2521; (b) Chen, Y. C.; Wu, T. F.; Deng, J. G.; Liu, H.; Cui, X.; Zhu, J.; Jiang, Y. Z.; Choi, M. C. K.; Chan, A. S. C. *J. Org. Chem.* **2002**, *67*, 5301; (c) Watanabe, M.; Murata, K.; Ikariya, T. *J. Org. Chem.* **2002**, *67*, 1712; (d) Sandoval, C. A.; Ohkuma, T.; Muñoz, K.; Noyori, R. *J. Am. Chem. Soc.* **2003**, *125*, 13490; (e) Jing, Q.; Zhang, X.; Sun, J.; Ding, K. *Adv. Synth. Catal.* **2005**, *347*, 1193; (f) Xia, Y. Q.; Tang, Y. Y.; Liang, Z. M.; Yu, C. B.; Zhou, X. G.; Li, R. X.; Li, X. J. *J. Mol. Catal. A: Chem.* **2005**, *240*, 132; (g) Mikami, K.; Wakabayashi, K.; Aikawa, K. *Org. Lett.* **2006**, *8*, 1517.
6. (a) Bergbreiter, D. E. *Chem. Rev.* **2002**, *102*, 3345; Lou, L.; (b) Liang, Y. X.; Jing, Q.; Li, X.; Shi, L.; Ding, K. *J. Am. Chem. Soc.* **2005**, *127*, 7694; (c) Liu, P. N.; Gu, P. M.; Wang, F.; Tu, Y. Q. *Org. Lett.* **2004**, *6*, 169; (d) Li, X. G.; Chen, W. P.; Hems, W.; King, F.; Xiao, J. L. *Org. Lett.* **2003**, *5*, 4559; (e) Peng, X. J.; Yu, K.; Liu, S. X. *Catal. Commun.* **2008**, *9*, 1891.
7. (a) Liu, G. H.; Yao, M.; Zhang, F.; Gao, Y.; Li, H. X. *Chem. Commun.* **2008**, 347; (b) Liu, G. H.; Yao, M.; Wang, G. Y.; Liu, M. M.; Zhang, F.; Li, H. X. *Adv. Synth. Catal.* **2008**, *350*, 1464.
8. (a) Liu, G. H.; Gao, Y.; Lu, X. Q.; Liu, M. M.; Zhang, F.; Li, H. X. *Chem. Commun.* **2008**, 3184; (b) Li, H. X.; Zhang, F.; Wan, Y.; Lu, Y. F. *J. Phys. Chem. B* **2006**, *110*, 22942; (c) Wan, Y.; Zhang, F.; Lu, Y. F.; Li, H. X. *J. Mol. Catal. A: Chem.* **2007**, *267*, 165; (d) Li, H. X.; Wu, Y. D.; Wan, Y.; Zhang, J.; Dai, W. L.; Qiao, M. H. *Catal. Today* **2004**, *93–95*, 493; (e) Li, H. X.; Zhao, Q. F.; Wan, Y.; Dai, W. L.; Qiao, M. H. *J. Catal.* **2006**, *244*, 251; (f) Li, H. X.; Bian, Z. F.; Zhu, J.; Huo, Y. N.; Li, H.; Lu, Y. F. *J. Am. Chem. Soc.* **2007**, *129*, 4538.
9. Chong, A. S. M.; Zhao, X. S. *J. Phys. Chem.* **2003**, *107*, 12650.
10. (a) Hu, Q. Y.; Hampsey, J. E.; Jiang, N.; Li, C. J.; Lu, Y. F. *Chem. Mater.* **2005**, *17*, 1561; (b) Chaplais, G.; Bideau, J. L.; Leclercq, D.; Vioux, A. *Chem. Mater.* **2003**, *15*, 1950.
11. Kröcher, O.; Köppel, O. A.; Fröba, M.; Baiker, A. *J. Catal.* **1998**, *178*, 284.
12. Zhao, D.; Huo, Q.; Feng, J.; Chmelka, B. F.; Stucky, G. D. *J. Am. Chem. Soc.* **1998**, *120*, 6024.
13. (a) Kruk, M.; Jaroniec, M.; Joo, S. H.; Ryoo, R. *J. Phys. Chem. B* **2003**, *107*, 2205; (b) Bao, X. Y.; Li, X.; Zhao, X. S. *J. Phys. Chem. B* **2006**, *110*, 2656.
14. (a) Xu, Y. J.; Alcock, N. W.; Clarkson, G. J.; Docherty, G.; Woodward, G.; Wills, M. *Org. Lett.* **2004**, *6*, 4105; (b) Xu, Y. J.; Clarkson, G. C.; Docherty, G.; North, C. L.; Woodward, G.; Wills, M. *J. Org. Chem.* **2005**, *70*, 8079.
15. (a) Burk, S.; Francio, G.; Leitner, W. *Chem. Commun.* **2005**, *27*, 3460; (b) Murahashi, F. I.; Takaya, H. *Acc. Chem. Res.* **2000**, *33*, 225; (c) Kuroki, Y.; Sakamaki, Y.; Iseki, K. *Org. Lett.* **2001**, *3*, 457; (d) Wu, X. F.; Vinci, D.; Ikariya, T.; Xiao, L. *Chem. Commun.* **2005**, 4447; (e) Xie, J. H.; Zhou, Q. L. *Acc. Chem. Res.* **2008**, *41*, 581.
16. (a) Mbaraka, I. K.; Shanks, B. H. *J. Catal.* **2005**, *229*, 365; (b) *Chem. Mater.* **1999**, *11*, 3285.